Optimal Under-Frequency Load Curtailment via Continuous Load Control in a Single Area Power System Using Fuzzy Logic, PID-Fuzzy and Neuro-Fuzzy (ANFIS) Controllers

Demilade D. Dinakin[a], Peter O. Oluseyi[b]

Department of Electrical and Electronics Engineering, University of Lagos, Akoka-Lagos, Nigeria
[a]e-mail: zemidinak@gmail.com
[b]e-mail: poluseyi@unilag.edu.ng

Abstract— In situations where maximum load demand exceeds power generation capacity, frequency would drop during cases of overload; and if appropriate under-frequency load curtailment scheme is not put in place, it could cause permanent turbine damage or affect the expected working operation of electric equipment. Various existing works on load curtailment in power systems have been done to great effect using meta-heuristic and classical control techniques. This paper seeks to comparatively analyze the Fuzzy Logic, Fuzzy-PID and Neuro-Fuzzy (ANFIS) controllers and their contribution to achieving load curtailment in a Single Area Power System via continuous load control. The transfer function model of the power system and the design of the controllers are done using Simulink, MATLAB software. The controllers are designed to output power imbalance based on frequency deviation during various system overload conditions. They also shed loads continuously until frequency is restored within the safe operating range. Different cases of system overload are used to analyze the performance of the controllers. It is found that the Neuro-Fuzzy controller gives the most optimized result.

Keywords— Classical control, load curtailment, meta-heuristic, under-frequency.

I. INTRODUCTION

The indicator of power system balance is the electric power frequency. Frequency stability depends on the ability to restore equilibrium between system generation and load demand with minimum loss of loads [1]. The frequency change during disturbances is depicted in Fig. 1.
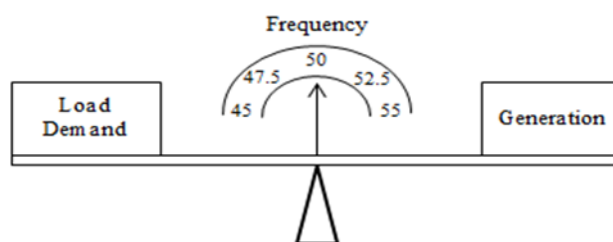

Fig. 1. Relationship between frequency and changes in load demand and generation

From Fig. 1, when demand exceeds generation, frequency decreases; and measures must be taken to restore frequency to its nominal level. This could affect the normal operation of electrical machines and appliances and create a need for load curtailment. C. Lui and others mentioned that "In 50 Hz electrical power systems, the frequency range during normal power system operation is a narrow band between 49.95 and 50.05 Hz; A frequency value outside this range normally calls for corrective control measures" [2]. These measures are done to control active power and frequency.

Under-frequency load shedding is one of the most important protection measures to prevent system collapse or total blackout. The frequency decay rate in situations of low-level power imbalances gives the turbine governor enough time to react accordingly. However, in cases of

higher levels of power imbalance, the mechanical turbine valves controlled by the turbine governor are too slow to react before the frequency falls below an acceptable limit [3].

Authors in [4] mentioned that "The objective of an under-frequency load shedding is to quickly recognize generation deficiency within any system and automatically shed a minimum amount of load, and at the same time provide a quick, smooth and safe transition of the system from emergency situation to a post-emergency condition such that a generation-load balance is achieved and nominal system frequency is restored".

There are various methods that have been used for load curtailment over the years. The earlier methods, which became the normal convention involved under-frequency relays and/or breaker interlocks schemes for system load shedding, are too slow as they do not effectively calculate the correct amount of load to be shed despite being later integrated with Programmable Logic Controllers [5].

More recently, however, meta-heuristic methods have been used for optimal load shedding among which include: the Ant Colony Optimization (ACO) technique [6], Fuzzy Logic Control (FLC) [7], [8], the Genetic Algorithm (GA) [9], Artificial Neural Network (ANN) [10]-[12], Adaptive Neuro-Fuzzy Inference System (ANFIS) [13]. Technique for Order Preference by Similarity to Ideal Solution (TOPSIS) [14], Cuckoo Search (CS) Algorithm [4], Firefly Algorithm (FA) [15] and Particle Swarm Optimization (PSO) [16], [17], Big Bang Big Crunch (BB-BC) [18], etc. These methods have proven to be very effective in achieving load curtailment in power systems.

Classical Control Design Techniques have also been used to achieve Load Curtailment [19], [20]. The classical controller design methodology is iterative; and it is effective for Single-Input, Single-Output (SISO), Linear Time-Invariant (LTI), system analysis and design [21]. Some of these controllers include: Proportional, Proportional-Integral (PI), Proportional-Integral-Derivative (PID) controllers,…etc.

Li. *et. al.* [22] carried out a research work on under-frequency load shedding using continuous load control. In this proposed scheme, the load shedding scheme was achieved by introducing a negative feedback, K, to shed loads based on the frequency deviation. Hence, the scheme was proven to be adaptive based on the negative feedback value, K. The adaptive nature of this scheme permits the introduction of a controller which would output power imbalance based on frequency deviation during various system disturbances. This research work seeks to replace this negative feedback with the following controllers, designed using meta-heuristic and classical control techniques: Fuzzy Logic Controller (FLC), Fuzzy-PID controller and Neuro-fuzzy (ANFIS) controller. This is done with a view to compare the performances of these controllers in achieving load curtailment via continuous load control while retaining the adaptive nature of the original proposed scheme. Basically, the intention is to minimize the performance index, J, as much as possible while satisfying frequency constraints.

The findings of this study will help ensure that the most optimal load curtailment scheme, based on the comparison made, is put in place for single area power systems in situations where the maximum load demand exceeds power generation capacity. This would restore balance between power generation and load demand, which would in turn prevent unwanted system collapse due to imbalance in such systems. Also, with more and more devices powered by power electronics and controlled by smart controllers, some loads such as electric vehicles, mass storage;…etc., can be controlled to change their power continuously [22]. Hence, if the most optimal frequency control scheme is put in place, it would guarantee performance improvement of such continuously controllable loads.

II.   METHODOLOGY

A) Transfer Function Representation of a Single Area Hydro Power System

The transfer function representation of a Single Area Hydro Power System is shown in Fig. 2; and is expressed as (1).
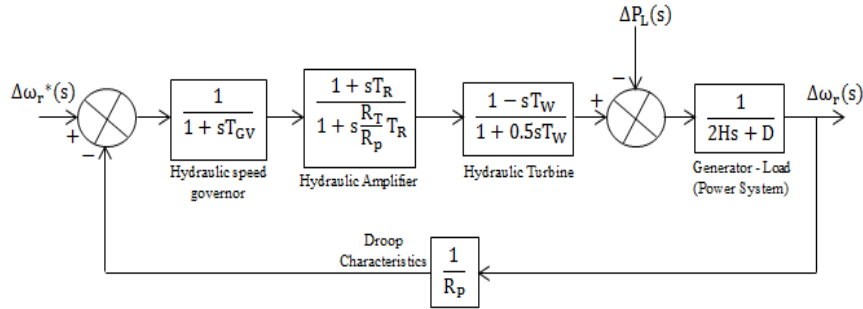

Fig. 2. Transfer function representation of a single area hydro-power system

$$\frac{\Delta\omega_r(s)}{-\Delta P_L(s)} = \frac{(sT_{GV}+1)(0.5sT_W+1)(sR_TT_R+R_P)}{(2Hs+D)(sT_{GV}+1)(0.5sT_W+1)(sR_TT_R+R_P)-(sT_R+1)(sT_W-1)} \tag{1}$$

The parameters used in the transfer function representation of the power system are shown in Table 1.

TABLE 1
TRANSFER FUNCTION SYSTEM PARAMETERS

Parameter	Symbol	Value	Unit
Servomotor Constant	T_{GV}	0.2	s
Permanent Droop	R_p	0.05	-
Water Starting Time	T_W	1	s
Inertia Constant	H	3.5	s
Load Damping Constant	D	1	pu

The temporary droop R_T is:

$$R_T = [2.3 - (1-1)0.15]\frac{1}{7} = \frac{2.3}{7} \text{ s} \tag{2}$$

The reset time T_R is:

$$T_R = [5 - (1-1)0.5]1 = 5 \text{ s} \tag{3}$$

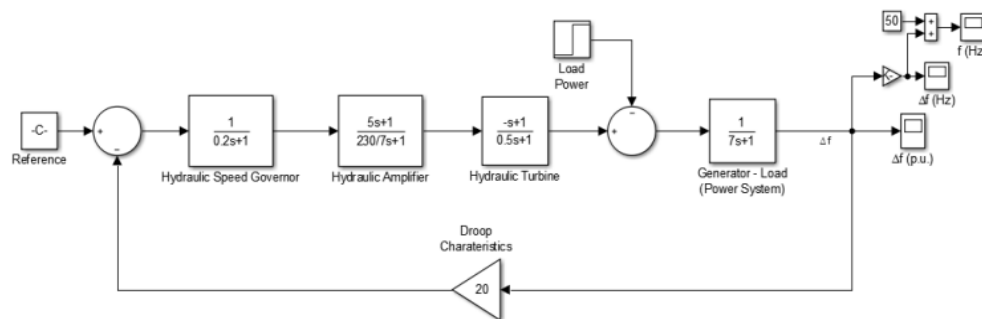The above system parameters are represented as shown in Fig. 3.

Fig. 3. The single area hydro power system transfer function

The transfer function of the system shown in Fig. 3 is as expressed in (4):

$$\frac{\Delta\omega_r(s)}{-\Delta P_L(s)} = \frac{0.1643s^3+1.155s^2+1.6779s+0.05}{1.1501s^4+8.2493s^3+7.9003s^2+6.0279s+1.05} \qquad (4)$$

B) Determining Power Imbalance by Load Shedding Sensitivity

As pointed out by Li. *et. al.* [22], there is a positive correlation between the amount of load shedding and the maximum frequency deviation. Load shedding sensitivity (LSS) is defined as the load shedding amount corresponding to per unit frequency deviation. This is shown in Fig. 4.
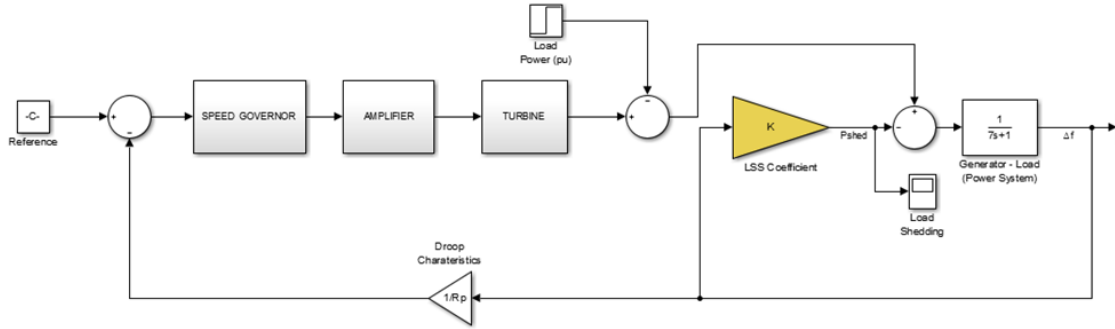

Fig. 4. Relationship between load shedding amount and frequency deviation

Therefore, the load sensitivity coefficient is given by (5) [7].

$$K = \frac{P_{shed}}{\Delta f} \qquad (5)$$

Where K is load sensitivity coefficient; Δf is maximum frequency deviation in pu; and P_{shed} is load shedding amount in pu.

From (5),

$$P_{shed} = K \times \Delta f \qquad (6)$$

The closed loop transfer function of the system with the load shedding sensitivity coefficient, K, is:

$$\frac{\Delta f(s)}{-\Delta P_L} = \frac{(sT_{GV}+1)(0.5sT_W+1)(sR_TT_R+R_P)}{(2Hs+D+K)(sT_{GV}+1)(0.5sT_W+1)(sR_TT_R+R_P)-(sT_R+1)(sT_W-1)} \qquad (7)$$

Therefore,

$$\Delta f(s) = \frac{-\Delta P_L}{2Hs+D+K-\delta} \qquad (8)$$

Where,

$$\delta = \frac{(sT_R+1)(sT_W-1)}{(sT_{GV}+1)(0.5sT_W+1)(sR_TT_R+R_P)} \qquad (9)$$

Substituting (8) in (6):

$$P_{shed} = \frac{-\Delta P_L \times K}{2Hs+D+K-\delta} \qquad (10)$$

$$\lim_{K\to\infty} P_{shed} = \frac{-\Delta P_L \times K}{2Hs+D+K-\delta} = -\Delta P_L \qquad (11)$$

Equation (11) shows that the total amount of load shed, P_{shed}, is equal to $-\Delta P_L$ as K tends to infinity. In other words, P_{shed} is always less than $-\Delta P_L$ whatever the value of K is; and there is no risk of over-shedding [22].

However, to eliminate shedding when frequency is still within normal operating range, the frequency threshold is used to determine maximum frequency deviation. Therefore,

$$\Delta f = \frac{f_{minimum} - f_{threshold}}{f_{nominal}} \tag{12}$$

Substituting (12) in (5), load shedding sensitivity coefficient becomes:

$$K = \frac{P_{shed} \times f_{nominal}}{f_{minimum} - f_{threshold}} \tag{13}$$

The under-frequency threshold for normal operation is 49.95 Hz. For 40% overload, the proportional gain is calculated as:

$$K = \frac{0.4 \times 50}{50 - 49.95} = 400 \tag{14}$$

This means that for a power imbalance of 40% and below, load shedding sensitivity of K=400 will adequately shed loads; and restore the system frequency within the range, 49.95Hz < f < 50Hz. However, for a fixed gain, K of 400, there would not be optimal load shedding for power imbalances less than 40%; hence, the design of the controllers is needed.

C) Designing the Fuzzy Logic Controller (FLC) for the System

Fuzzy Logic Control is described by a knowledge-based Algorithm. A Fuzzy Control System (FCS) basically involves three stages. They include Fuzzification, Fuzzy Inference Process and Defuzzification as shown in Fig. 5.
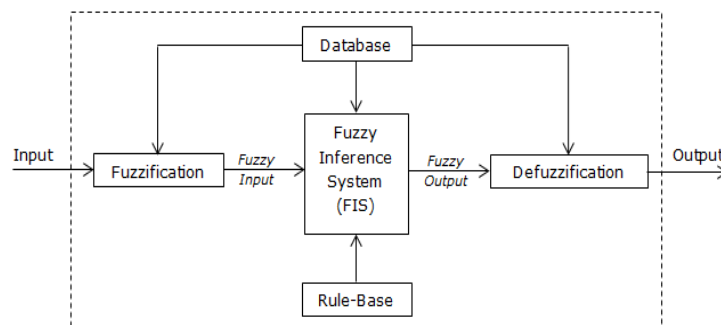

Fig. 5. A typical fuzzy control system

C.1. Fuzzification

It involves mapping input and output variables into membership functions. The triangular membership function (TRIMF) is used to map both input and output variables. The frequency deviation in per unit (pu), which results from system overload, is taken as the input variable; and it is mapped into 23 membership functions as shown in Fig. 6.
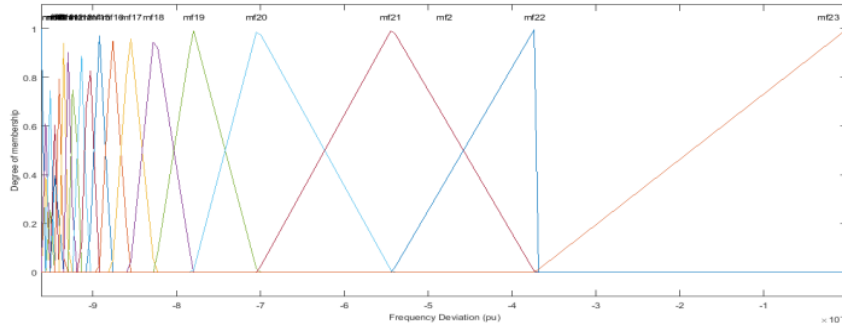
Fig. 6. Fuzzification of the input variable

Power Imbalance is taken as the output variable; and is mapped into 23 membership functions as shown in Fig. 7.
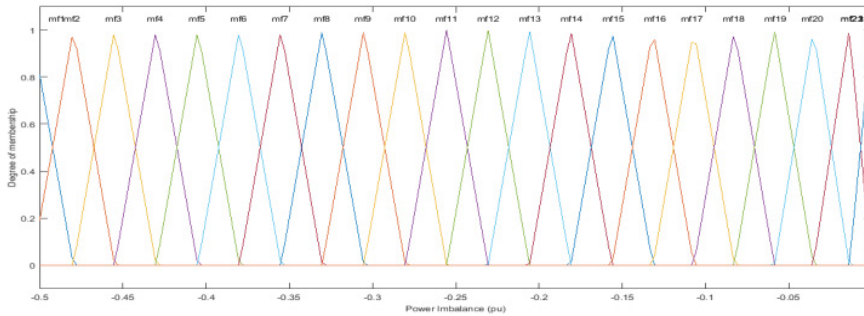

Fig. 7. Fuzzification of the output variable

C.2. Fuzzy Inference Process

The Algorithm requires 23 Fuzzy control rules based on input and output membership functions. The Mamdani-type FLS rule structure is used to operate the Fuzzy combination. The input is mapped into an output using a set of if-then rules. Based on the rules, the plot of the dependency of the output on the input is shown in Fig. 8.
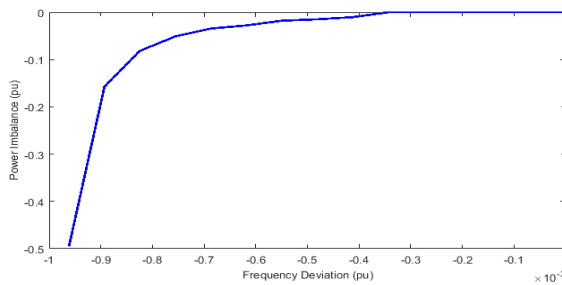

Fig. 8. Fuzzification of the output variable

C.3. Fuzzy Inference Process

This is the final stage in Fuzzy Control System design. It involves converting the Fuzzy Output into a quantifiable value. There are various methods used in defuzzification with the Center of Gravity (COG) being one of the most widely used methods. The COG method is adopted in designing the Fuzzy Control System. It is expressed by (15).

$$x^* = \frac{\sum_{i=1}^{N} A_i \times \overline{x_i}}{\sum_{i=1}^{N} A_i}$$
(15)

Where N is the number of sub-areas; A_i is the area of ith sub-area; $\overline{x_i}$ is the centroid of area of ith sub-area; and x^* is the defuzzified value (Output).

D) Designing the Fuzzy-PID Controller for the System

The Fuzzy-PID Controller combines the FLC with the PID controller to create a hybrid controller. The Fuzzy interface is used to calculate the values of the PID control parameters (K_P, K_I, K_D). Therefore, it works as an automatic tuner for the PID controller [23]. A typical Fuzzy-PID controller is shown in Fig. 9.
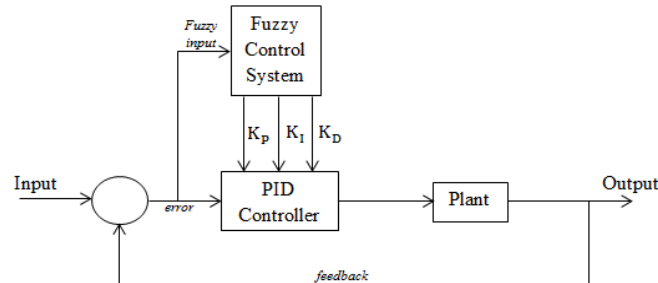

Fig. 9. A typical fuzzy-pid controller (hybrid controller)

The Fuzzy-PID controller for the system is designed by taking the deviation of the frequency of the system as an input to the FLC while the output of the FLC is the proportional, integral and derivative gains of the PID controller. The fuzzification of input and output variables is done using 23 triangular membership functions. These are shown in Figs 10-13.
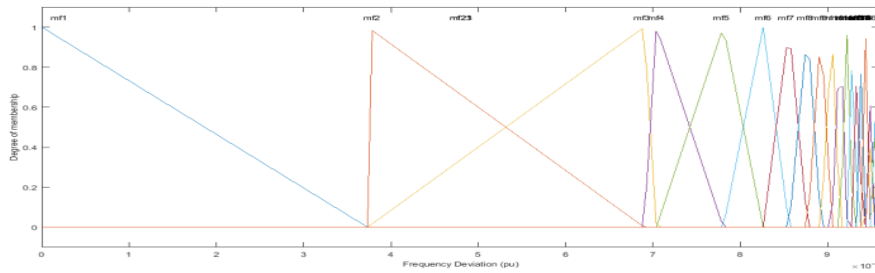

Fig. 10. Fuzzification of the input variable (frequency deviation)
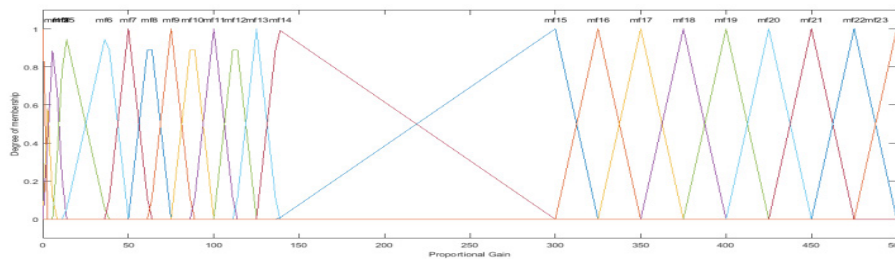

Fig. 11. Fuzzification of the output variable (proportional gain)
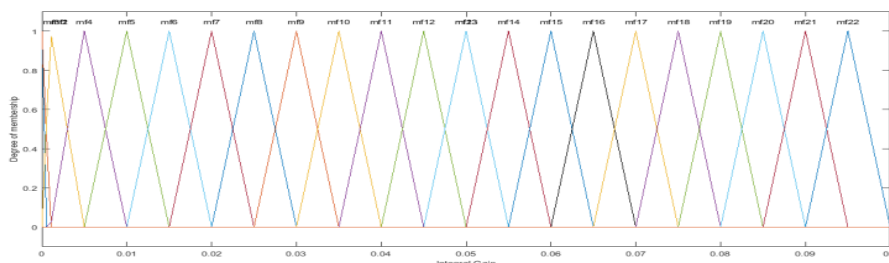

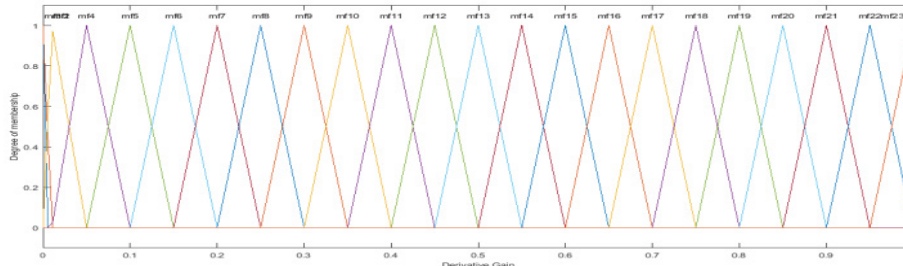Fig. 12. Fuzzification of the output variable (integral gain)

Fig. 13. Fuzzification of the output variable (derivative gain)

The system is designed using 23 rules to relate the input variable with the output variables. The Mamdani-type FLS rule structure is used to operate the Fuzzy combination. The rules create a relationship between the input and output variables. This relationship is depicted by the curves shown in Fig. 14.
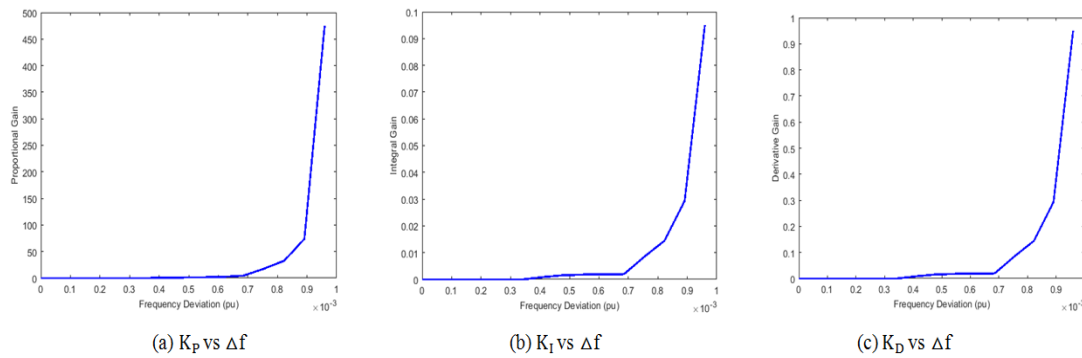

(a) K_P vs Δf (b) K_I vs Δf (c) K_D vs Δf

Fig. 14. Relationship between the input and output variables

E) Designing the Neuro-Fuzzy (ANFIS) Controller for the System

Authors in [24] mentioned that "ANFIS uses a hybrid learning algorithm to identify the membership function parameters of single-output, Sugeno type fuzzy inference systems (FIS). A combination of least-squares and back propagation gradient descent methods are used for training FIS membership function parameters to model a given set of input/output data". The design of the ANFIS controller is also done using MATLAB software. Some data (frequency deviation and power imbalance) were extracted from the P_{shed} output due to the Load Shedding Sensitivity (LSS) coefficient, K on the system. This is taken as the training data which require a training algorithm to make the ANFIS output match the training data. The Gaussian membership function is used in the design while the hybrid optimization method is used as the training algorithm with zero error tolerance and an epoch of 10. Training is done using the Neuro-Fuzzy Designer interface shown in Fig. 15.
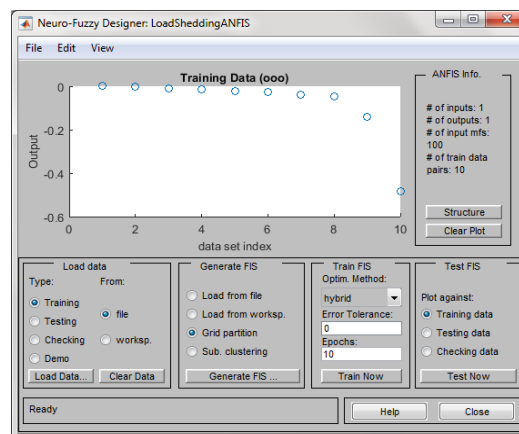

Fig 15. Training the ANFIS data using the neuro-fuzzy designer interface

The network required a total of 100 rules for an accurate ANFIS output. The architecture of the designed ANFIS model is shown in Fig. 16.
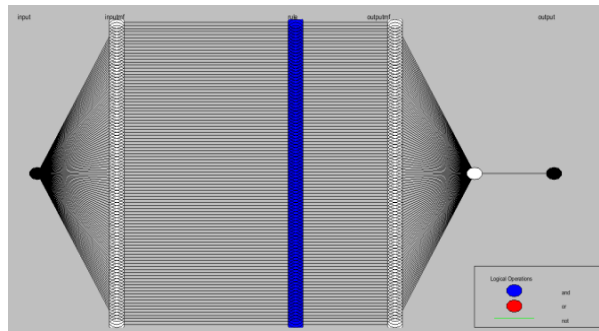
Fig. 16. Architecture of the designed ANFIS model

The Root Mean Square Error (RMSE) before training, as calculated using MATLAB syntax, is 0.1062. The plots of the ANFIS output against the training data before and after training are shown in Fig. 17.
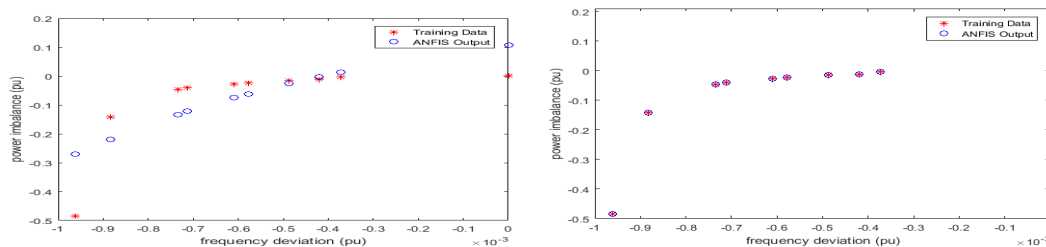
Fig. 17. Plots of the ANFIS output against the training data before and after training

The RMSE after training, as calculated using MATLAB syntax, is 3.052×10^{-3}. The plot of the ANFIS controller output (Power Imbalance) against ANFIS controller input (frequency deviation) is shown in Fig. 18.
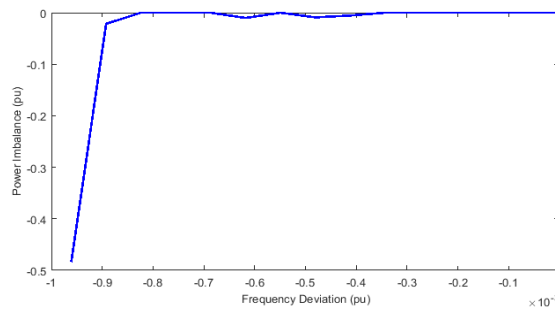
Fig. 18. Plot of the ANFIS output against the input

Each controller is placed in the Single Area Hydro Power system as shown in Fig. 19.

Fig. 19. Overall system with controller

The under frequency load shedding algorithm for continuous load control is shown in Fig. 20.
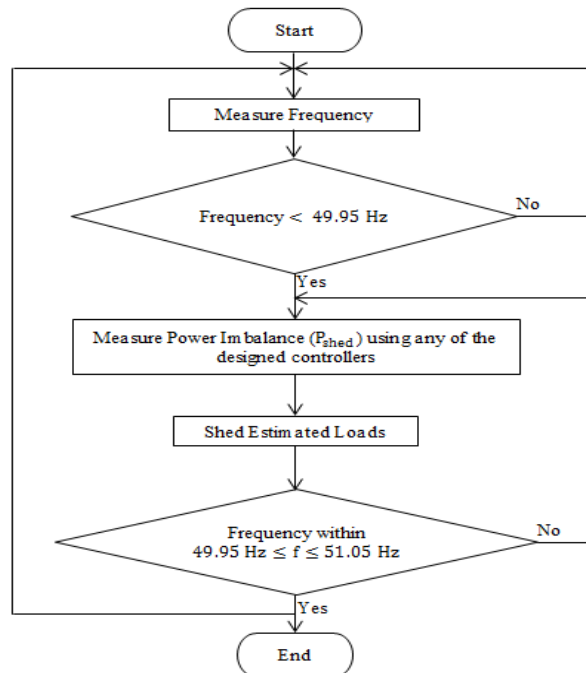
Fig. 20. Continuous under frequency load shedding algorithm

III.   RESULTS AND DISCUSSION

The controllers are designed because the governor action is too slow to act in extreme overload situations. Thus, they cannot adequately restore frequency within the nominal operating range. Fig. 21 shows the frequency response for a 40% system overload without a controller. The system was subjected to an overlo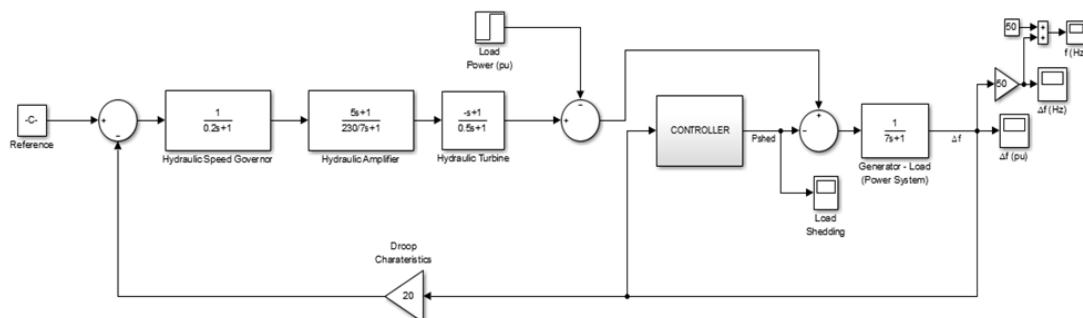ad after 5 seconds. It has been observed that frequency dropped to a maximum low of 43.97 Hz after 2.86 seconds from the time of overload. Eventually, the system was restored to a steady state frequency of 49.05 Hz after around 20 seconds. Hence, it takes over 20 seconds for the turbine to restore the system within a steady frequency value for an overload of 40%, which is not even within the normal frequency operating range. However, it should be noted that deviation in the frequency of the power system after a governor takes an action does not mean there is a lack of power generation. Rather it is due to the characteristics of the governor, especially when the frequency deviation is small.

Fig. 21. Frequency response for a 40% system overload

Table 2 below shows the estimated Power Imbalance (PI) in per unit (pu) and frequency deviation (△f) in Hertz (Hz) of the three designed controllers for system overload varying from 1% to 40%.

TABLE 2

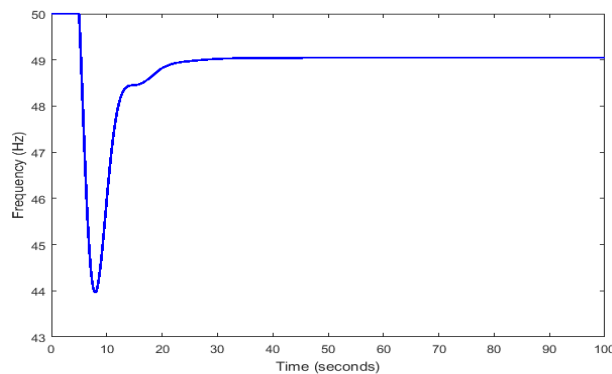ESTIMATED POWER IMBALANCE OF THE CONTROLLERS AND FREQUENCY DEVIATION DURING OVERLOADING CONDITIONS

Over Load, pu	Controllers					
	Fuzzy		Fuzzy-PID		ANFIS	
	PI, pu	Δf, Hz	PI, pu	Δf, Hz	PI, pu	Δf, Hz
0.01	-0.0157	-0.02599	-0.0006	-0.02237	-0.0018	-0.02046
0.02	-0.0080	-0.01984	-0.0058	-0.03525	-0.0086	-0.02837
0.03	-0.0188	-0.02770	-0.0145	-0.03808	-0.0159	-0.03512
0.04	-0.0275	-0.03075	-0.0238	-0.04032	-0.0259	-0.03520
0.05	-0.0359	-0.03521	-0.0332	-0.04191	-0.0310	-0.04744
0.06	-0.0453	-0.03659	-0.0429	-0.04272	-0.0410	-0.04750
0.07	-0.0546	-0.03841	-0.0525	-0.04353	-0.0525	-0.04384
0.08	-0.0647	-0.03943	-0.0623	-0.04415	-0.0624	-0.04387
0.09	-0.0737	-0.04049	-0.0721	-0.04474	-0.0724	-0.04389
0.10	-0.0834	-0.04135	-0.0819	-0.04523	-0.0824	-0.04392
0.11	-0.0932	-0.04192	-0.0917	-0.04560	-0.0924	-0.04394
0.12	-0.1029	-0.04260	-0.1016	-0.04594	-0.1024	-0.04397
0.13	-0.1128	-0.04300	-0.1115	-0.04620	-0.1124	-0.04399
0.14	-0.1226	-0.04350	-0.1214	-0.04645	-0.1224	-0.04403
0.15	-0.1325	-0.04388	-0.1314	-0.04645	-0.1309	-0.04769
0.16	-0.1423	-0.04418	-0.1414	-0.04646	-0.1409	-0.04770
0.17	-0.1522	-0.04453	-0.1514	-0.04646	-0.1509	-0.04771
0.18	-0.1621	-0.04475	-0.1614	-0.04647	-0.1609	-0.04772
0.19	-0.1720	-0.04504	-0.1714	-0.04649	-0.1709	-0.04773
0.20	-0.1819	-0.04526	-0.1813	-0.04674	-0.1809	-0.04774
0.21	-0.1918	-0.04545	-0.1913	-0.04678	-0.1909	-0.04774
0.22	-0.2017	-0.04567	-0.2013	-0.04681	-0.2009	-0.04775
0.23	-0.2117	-0.04581	-0.2113	-0.04684	-0.2109	-0.04776
0.24	-0.2216	-0.04600	-0.2212	-0.04687	-0.2209	-0.04777
0.25	-0.2315	-0.04614	-0.2312	-0.04690	-0.2309	-0.04777
0.26	-0.2415	-0.04627	-0.2412	-0.04694	-0.2409	-0.04778
0.27	-0.2514	-0.04641	-0.2512	-0.04709	-0.2509	-0.04779
0.28	-0.2614	-0.04651	-0.2611	-0.04713	-0.2609	-0.04780
0.29	-0.2713	-0.04664	-0.2711	-0.04715	-0.2709	-0.04780
0.30	-0.2813	-0.04674	-0.2811	-0.04716	-0.2809	-0.04781
0.31	-0.2913	-0.04683	-0.2911	-0.04716	-0.2909	-0.04782
0.32	-0.3012	-0.04694	-0.3011	-0.04717	-0.3009	-0.04783
0.33	-0.3112	-0.04701	-0.3111	-0.04719	-0.3109	-0.04783
0.34	-0.3211	-0.04710	-0.3211	-0.04723	-0.3209	-0.04784
0.35	-0.3311	-0.04718	-0.3311	-0.04731	-0.3309	-0.04785
0.36	-0.3411	-0.04250	-0.3410	-0.04737	-0.3408	-0.04786
0.37	-0.3511	-0.04733	-0.3510	-0.04743	-0.3508	-0.04786
0.38	-0.3621	-0.04739	-0.3610	-0.04750	-0.3608	-0.04787
0.39	-0.3710	-0.04746	-0.3710	-0.04755	-0.3708	-0.04788
0.40	-0.3810	-0.04751	-0.3809	-0.04761	-0.3808	-0.04789

To better display the data in Table 2, Fig. 22a shows the chart of the controller's outputs of estimated power imbalance for overloads of 10% to 40%. The frequency deviation resulting from each controller action for overloads of 1% to 40% varied over 1% is shown in Fig. 22b.

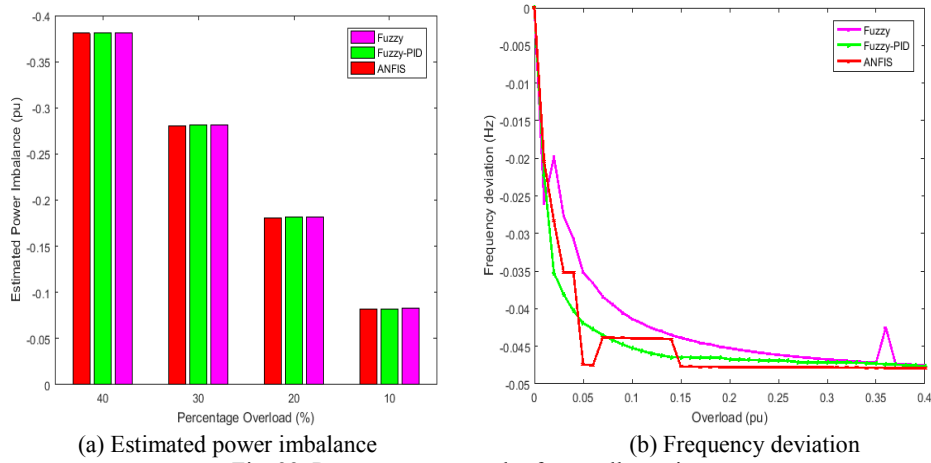(a) Estimated power imbalance   (b) Frequency deviation
Fig. 22. Responses as a result of controller action

In order to establish a comparative analysis, three scenarios are taken into consideration. The first case study is a situation in which the system is subjected in succession to an increasing overload. The second case study is a situation in which the system is subjected in succession to a decreasing overload. The third case scenario is a situation in which the system is subjected to random overloads at different points in time.

For case study 1, Fig. 23 shows the responses of each controller to an increasing overload. The system is subjected to an overload of 5% after 5 seconds. This was increased by 5% over an interval of 5 seconds up till 40% overload. The frequency responses are thus shown as follows:

(a) FLC   (b) Fuzzy-PID   (c) ANFIS
Fig. 23. Frequency response using the controllers for case study one

For case study 2, Fig. 24 shows the responses of each controller to a decreasing overload. The system is subjected to an overload of 40% after 5 seconds. This is decreased by 5% over an interval of 5 seconds. The frequency responses are thus shown as follows:

(a) FLC   (b) Fuzzy-PID   (c) ANFIS
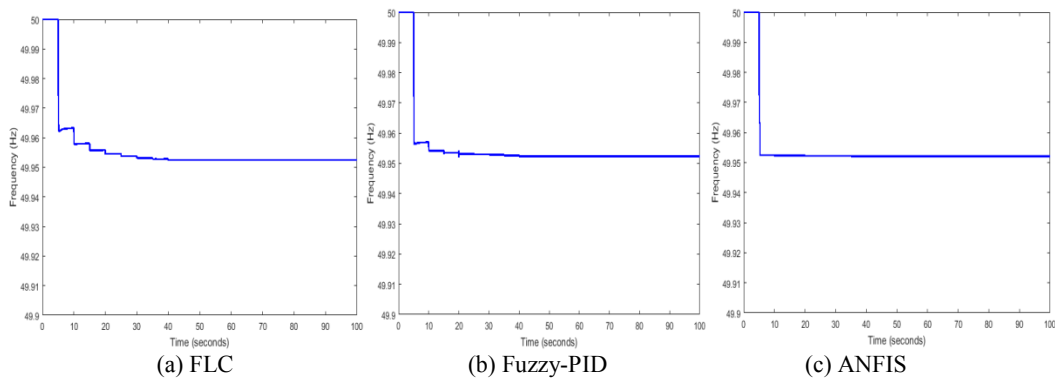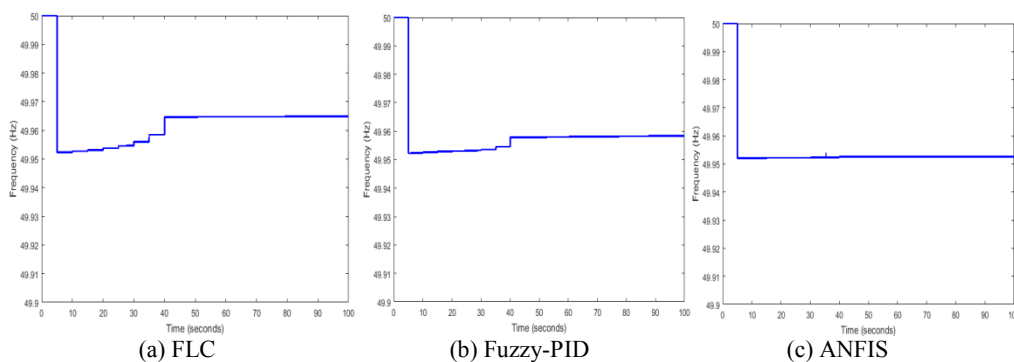Fig. 24. Frequency response using the controllers for case study two

For case study 3, Fig. 25 shows the responses of each controller to a random overload. The system is initially subjected to an overload of 20% after 5 seconds. This overload is varied randomly after intervals of 5 seconds. The frequency responses are thus shown as follows:

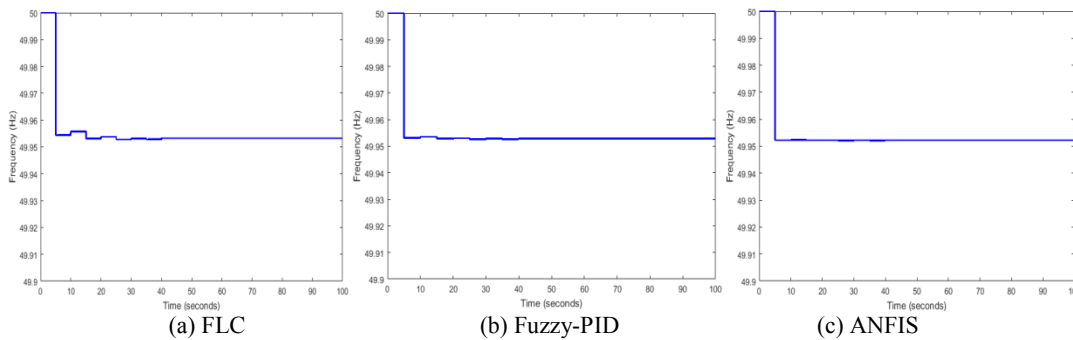(a) FLC   (b) Fuzzy-PID   (c) ANFIS
Fig. 25. Frequency Response using the ANFIS controller for case study three

The performance indices used for the controller comparison include: Integral Square Error (ISE), Integral Absolute Error (IAE), Integral Time Square Error (ITSE) and Integral Time Absolute Error (ITAE). The error signal in this case is the estimated Power Imbalance (P_{shed}) by controllers. The lower the performance index, J, the better the performance of the designed controller in shedding optimal load amounts while maintaining frequency within the normal operating range. In other words, the controllers were designed to minimize J, subject to the constraint, $f_{min} \leq f \leq f_{max}$. Where f_{min} is 49.95 Hz; and f_{max} is 50.05Hz.
Performance indices of the controllers for each case study are summarized in Table 3.

TABLE 3
PERFORMANCE INDICES OF EACH CONTROLLER FOR DIFFERENT CASE SCENARIOS

Case Studies	Controllers	Performance Indices			
		ISE	IAE	ITSE	ITAE
1	FLC	10.41	29.68	664.1	1792
	Fuzzy-PID	10.39	29.64	663.3	1790
	ANFIS	10.38	29.62	662.5	1789
2	FLC	2.478	10.59	42.06	304.9
	Fuzzy-PID	2.471	10.48	41.49	296.5
	ANFIS	2.470	10.39	41.15	289.7
3	FLC	7.372	26.16	402.8	1413
	Fuzzy-PID	7.363	26.14	402.3	1412
	ANFIS	7.355	26.12	401.8	1411

The single area power system was modeled in the transfer function representation using MATLAB software. During full load operation, the system frequency was at 50Hz. However, when the system was subjected to an overload, frequency began to drop. For instance, the system was subjected to a 40% overload; and frequency dropped to 43.97 Hz after only 2.86 seconds. Although the turbine action attempted to restore frequency to a safe operating range, frequency was only restored to a steady state of 49.05 Hz after over 20 seconds. This slow reaction of the turbine led to the design of controllers that quickly act on frequency drop and maintain frequency within the nominal operating range.
The controllers were designed to shed loads continuously during various overload conditions. The overload was initially varied from 1% to 40%. The estimated Power Imbalances and frequency deviation of each controller were observed. The expected frequency deviation was

not supposed to exceed ±0.05 Hz. It was seen that the ANFIS controller shed the least Power for every overload situation. This was followed by the Fuzzy-PID controller and then the FLC. Three cases were taken into consideration while testing the controllers. The first scenario describes a situation in which the system was subjected to an increasing overload. The system was subjected to a 5% overload every 5 seconds; and it was increased by 5% after every 5 seconds until a 40% overload. The controllers maintained frequency within the nominal operating range of 49.95 Hz ≤ f ≤ 50.05 Hz during the whole period. Case study 2 was a situation in which the system is subjected to a decreasing overload. The system was initially subjected to a 40% overload after 5 seconds. Then this overload was decreased by 5% after a 5-second interval until there was no system overload. As seen in figure 3.4, the FLC, Fuzzy-PID and ANFIS controllers maintained frequency within the nominal operating range of 49.95 Hz ≤ f ≤ 50.05 Hz during the whole period. The final case study described a situation in which the system was subjected to random overloads. The system was subjected to random overloads at intervals of 5 seconds. Again, the controllers maintained frequency within the nominal operating range of 49.95 Hz ≤ f ≤ 50.05 Hz during the whole period.

The performance indices, ISE, IAE, ITSE and ITAE, were used to comparatively analyze the designed controller for the most minimized performance index. Over the three case studies, the ANFIS controller resulted in the most reduced performance index. In other words, the ANFIS controller was shedding the least power while maintaining system frequency within the nominal operating range. This was closely followed by the Fuzzy-PID controller and the FLC, respectively.

IV. CONCLUSION

This paper has presented optimal under-frequency load curtailment via continuous load control for a Single Area Power System. The scheme used frequency deviation to estimate load imbalance and shed load continuously until frequency was restored within a safe operating range. Three different controllers were designed to help achieve this; and were comparatively analyzed by using various performance indices. The controllers include: FLC, Fuzzy-PID and Neuro-Fuzzy controllers. The Single Area Power System, together with the controllers, was modeled using the Simulink, MATLAB software. The system was subjected to various overload conditions. Results showed that the ANFIS controller was most optimal among all three controllers. Nevertheless, the Fuzzy-PID controller had almost similar values to the ANFIS controller which was closely followed by the FLC. Future work will be to further carry out the performance comparison of these controllers in a Multi-Area (Hydro, Thermal or Hydro-Thermal) Power System, where each single area has an individual generator or a number of generators that are closely coupled to form a coherent group.

REFERENCES

[1] P. Kundur, J. Paserba, V. Ajjarapu, G. Andersson, A. Bose, C. Canizares, N. Hatziargyriou, D. Hill, A. Stankovic, C. Taylor, T. Van Cutsem, and V. Vittal, "Definition and classification of power system stability IEEE/CIGRE joint task force on stability terms and definitions," *IEEE Transactions on Power Systems*, vol. 19, no. 3, pp. 1387-1401, 2004.

[2] C. Liu, S. McArthur, and S. Lee, *Smart Grid Handbook*, Hoboken, NJ: Wiley, 2016.

[3] U. Rubez and R. Mihalic, "Analysis of under-frequency load shedding using a frequency gradient," *IEEE Transactions on Power Delivery*, vol. 26, no. 2, pp. 565-575, 2011.

[4] C. Mwaniki, C. Muriithi, N. Abungu, and G. Nyakoe, "Optimal under-frequency load shedding using cuckoo search with levy flight algorithm for frequency stability improvement," *International Journal of Emerging Technology and Advanced Engineering*, vol. 5, no. 10, pp. 8-14, 2015.

[5] F. Shokooh, J. Dai, S. Shokooh, J. Taster, H. Castro, T. Khandelwal, G. Donner, "An intelligent load shedding (ILS) system application in a large industrial facility," *Proceedings of Conference Record of the 2005 IEEE Industry Applications Conference Fortieth IAS Annual Meeting*, vol. 1, pp. 417-425, 2005.

[6] W. Nakawiro and I. Erlich, "Optimal load shedding for voltage stability enhancement by ant colony optimization," *Proceedings of 5th International Conference on Intelligent System Applications to Power Systems*, pp. 1-6, 2009.

[7] H. Cimen and M. Aydin, "Optimal load shedding strategy for Selçuk university power system with distributed generation," *Procedia–Social and Behavioral Sciences,* vol. 195, pp. 2376-2381, 2015.

[8] J. Kaewmanee, S. Sirisumrannukul, and T. Menaneanatra, "Optimal load shedding in power system using fuzzy decision algorithm," *Proceedings of AORC-CIGRE Technical meeting 2013*, vol. 5, no. 5, pp. 43-61, 2013.

[9] C. Chen, W. Tsai, H. Chen, C. Lee, C. Chen, and H. Lan, "Optimal load shedding planning with genetic algorithm," *Proceedings of IEEE Industry Applications Society Annual Meeting*, pp. 1-6, 2011.

[10] F. Muhammad, T. Hafiz, M. Kashif, G. Hafiz, and R. Umair, "Optimal load shedding using an ensemble of artificial neural networks," *Electrical and Computer Engineering Systems*, vol. 7, no. 2, 2016.

[11] B. Suneetha, S. Hemachandra, B. Prasad, and A. Jayanth, "Application of neural network in load shedding and some predictable functioning of load shedding methods," *Electronics, Communication & Instrumentation Engineering Research and Development*, vol. 3, no. 2, pp. 45-50, 2013.

[12] N. Trong, A. Ngoc, A. Huy, and B. Thanh, "Load shedding control strategy based on transient instability evaluation of power system using artificial neural network and analytic hierarchy process algorithm," *Preprints*, pp. 1-14, 2017.

[13] M. Dreidy, H. Mokhlis, and S. Mekhilef, "A new under-frequency load shedding scheme based on adaptive neuro-fuzzy inference system and evolutionary programming shedding priority," *Proceedings of IOP Conference Series: Earth and Environmental Science*, vol. 164, 2018.

[14] H. Goh and A. Zin, "Combination of TOPSIS and AHP in load shedding scheme for large pulp mill electrical system," *Electrical Power & Energy Systems*, vol. 47, pp. 198-204, 2013.

[15] V. Sonar and V. Shaikh, "Optimal load shedding for power system using firefly algorithm," *International Journal for Scientific Research & Development*, vol. 3, no. 3, pp. 3492-3495, 2015.

[16] M. Dreidy, H. Mokhlis, and S. Mekhilef, "Application of meta-heuristic techniques for optimal load shedding in islanded distribution network with high penetration of solar PV generation," *Energies*, vol. 10, no. 2, pp. 1-24, 2017.

[17] R. Hooshman, "Optimal design of load shedding and generation reallocation (LSGR) in power systems using fuzzy particle swarm optimization (FPSO) algorithm," *Applied Sciences*, vol. 8 no. 16, pp. 2788-2800, 2008.

[18] F. Kucuktezcan and I. Genc, "Optimal load shedding scheme in power systems based on big bang big crunch method," *Proceedings of the IASTED International Conference on Power and Energy Systems and Applications (PESA)*, no. 756-071, 2011.

[19] D. Tyagi, A. Kumar, and S. Chanana, "Load shedding via PID controller for an isolated power system," *Proceedings of IEEE Fifth Power India Conference*, pp. 1-6, 2012.

[20] S. Singh, D. Tyagi, A. Kumar, and S. Chanana, "Load shedding in deregulation environment and impact of photovoltaic system with SMES," *Energy Procedia,* vol. 90, pp. 412-422, 2016.

[21] W. Zhong, *Duality System in Applied Mechanics and Optimal Control*, Manhattan, NY: Springer US, 2004.

[22] C. Li, Y. Sun and Y. Yu, "An under-frequency load shedding scheme with continuous load control proportional to frequency deviation," *Proceedings of IOP Conference Series: Materials Science and Engineering*, vol. 199, no. 012074, 2017.

[23] S. Jain and N. Beniwal, "Hybrid PID-fuzzy controlling approach," *Advanced Research in Electronics and Communication Engineering,* vol. 4, no. 11, pp. 2648-2651, 2015.

[24] MATLAB. Natick, Massachusetts: The MathWorks, Inc., version 9.0.0.341360, 2016.